Intraband absorption of doped GaN/AlN quantum dots at telecommunication wavelengths

M. Tchernycheva,[a] L. Nevou, L. Doyennette, A. Helman, R. Colombelli, and F. H. Julien
Opération Transversale OptoGaN, Institut d'Electronique Fondamentale, UMR 8622 CNRS, Université Paris-Sud, 91405 Orsay cedex, France

F. Guillot and E. Monroy
Equipe mixte CEA-CNRS-UJF Nanophysique et Semiconducteurs, DRFMC/SP2M/PSC, CEA-Grenoble, 17 rue des Martyrs, 38054 Grenoble cedex 9, France

T. Shibata and M. Tanaka
NGK Insulators, Limited, 2-54 Sudacho, Mizuhoku, Nagoya Japan

(Received 14 April 2005; accepted 27 July 2005; published online 2 September 2005)

We report the Stranski–Krastanov growth of Si-doped GaN/AlN quantum dot superlattices displaying conduction-band interlevel absorption at telecommunication wavelengths. By adjusting the growth conditions, quantum dots with a height of 0.5–1 nm in the density range of 0.1×10^{12}–3×10^{12} cm^{-2} can be synthesized. All of the samples exhibit room-temperature interlevel absorptions in the 1.41–1.54 μm wavelength range. The full width at half maximum of the observed intraband absorptions is as small as 88 meV. We also observe residual intraband absorption for nominally undoped samples. We attribute this effect to the detrapping of electrons in the AlN barriers and subsequent capture in the dots. © *2005 American Institute of Physics*.
[DOI: 10.1063/1.2042540]

Semiconductor heterostructures based on group-III nitrides are promising candidates for unipolar intersubband (ISB) devices operating at fiber-optics telecommunication wavelengths. Thanks to their large conduction-band offset—which, for instance, is of the order of 1.7 eV at the GaN/AlN heterointerface—ISB transitions in the 1–3 μm wavelength range can be obtained. So far, several groups have observed ISB absorption at 1.3–1.55 μm wavelength in GaN/AlGaN quantum wells grown by molecular-beam epitaxy (MBE).[1–5] In addition, interlevel absorptions in the conduction band of nonintentionally doped (n.i.d.) hexagonal-phase GaN/AlN quantum dots (QDs) have recently been reported.[6] Under optical excitation by an ultraviolet (UV) laser, QDs with a height along the c axis of $z\approx4.5$ nm and an in-plane diameter of 22 nm exhibit s-p_x and s-p_z intraband transitions, respectively, peaked at 0.15 eV ($\lambda\approx8.3$ μm) and 0.6 eV ($\lambda\approx2.1$ μm).[6,7] In order to achieve shorter wavelengths, the dot height must be reduced to approximately 1 nm.[8] It is also desirable to populate the dots with electrons through proper n doping, since many potential device applications—such as QD photodetectors, optical switches, or modulators—require a populated ground state. The n doping of GaN/AlN QDs has not been demonstrated yet.

In this work, we present the growth of Si-doped GaN/AlN QD superlattices. The samples exhibit room-temperature intraband absorptions peaked at wavelengths ranging from 1.41 μm to 1.54 μm, i.e., within the fiber-optics telecommunication wavelength band. The full width at half maximum (FWHM) of this absorption is as small as 88 meV.

The samples investigated in this work consist of 20 periods of GaN QD layers with 3-nm-thick AlN barriers, grown by plasma-assisted MBE on 1-μm-thick AlN-on-sapphire (0001) templates. An additional QD plane was deposited on the surface to allow atomic force microscopy (AFM) characterization of the QD shapes and density. The QDs are formed by deposition of 4 monolayers (ML) of GaN on an AlN surface under nitrogen-rich conditions. Under these conditions, the growth starts layer by layer, leading to a 2 ML GaN wetting layer. Further deposition of GaN leads to the formation of three-dimensional islands (Stranski–Krastanov growth mode).[9,10] The QD formation was monitored *in situ* by reflection high-energy electron diffraction (RHEED), which showed a rapid increase of the a-axis lattice parameter and of the RHEED intensity after the deposition of the 2-ML-thick wetting layer. The synthesis of each GaN QD plane is followed by a growth interruption (GI) under a vacuum, during which additional reflections corresponding to the QD facets become visible in the RHEED pattern. These GaN QDs are hexagonal truncated pyramids with {1-103} facets,[11] and no Ga–Al interdiffusion has been observed.[12] The substrate temperature was kept at an intentionally low value of 720 °C to limit the capture radius around the QDs and thus reduce the QD height, while at the same time increasing the QD density. Doping was introduced in the QDs by opening the Si cell during the growth of the GaN layers. The doping level was calibrated for several Si-cell temperatures by performing Hall measurements on micrometer thick GaN layers. The doping level and GI time after each QD plane, as well as the QD density and sizes for all the investigated samples, are summarized in Table I.

Figure 1 shows the AFM image of the QD plane synthesized on the surface of Sample E644. The QD density is very high (1.2×10^{12} cm^{-2}) and the average QD height is about 1 nm. AFM measurements have not revealed any significant effect of Si doping on the QD shape. The size of the QDs can be tuned by adjusting the GI time after the QD formation, which results in a decrease in their density and an increase in

[a]Author to whom correspondence should be addressed; electronic mail: maria.tchernycheva@ief.u-psud.fr

TABLE I. Sample growth parameters (doping level and GI time), QD heights (above the 0.5-nm-thick wetting layer), diameter and density estimated from AFM measurements, experimental PL energy and FWHM, intraband peak energy, FWHM, and absorption per reflection. All of the measurements have been performed at room temperature.

Sample No.	Doping (cm^{-3})	GI time	QD height (diameter) (nm)	QD density (cm^{-2})	Intraband energy (FWHM) (eV)	Absorption per reflection (%)	PL (FWHM) (eV)
E645	n.i.d.	15 s	$1.3\pm0.6(11\pm2)$	$1.2\pm0.1\times10^{12}$	0.823 (0.094)	1.4	3.826 (0.195)
E646	1.1×10^{19}	15 s	$1.3\pm0.6(10\pm2)$	$1.1\pm0.1\times10^{12}$	0.826 (0.094)	2.4	3.824 (0.195)
E644	1×10^{20}	15 s	$1.3\pm0.6(11\pm5)$	$1.2\pm0.6\times20^{3}$	0.837 (0.112)	5.1	3.818 (0.261)
E649	1×10^{20}	0 s	$0.9\pm0.4(11\pm2)$	$2.9\pm0.1\times10^{12}$	0.878 (0.088)	3.1	3.894 (0.246)
E647	1×10^{20}	1 min	$1.2\pm0.6(20\pm3)$	$4\pm0.4\times10^{11}$	0.823 (0.1)	3.8	3.82 (0.24)
E648	1×10^{20}	2 min	$1.5\pm0.7(28\pm2)$	$1\pm0.2\times10^{11}$	0.81 (0.125)	5.2	3.816 (0.237)

their diameter. This process is known as "Ostwald ripening". Indeed, the data in Table I show how the QD diameter evolves from 10 ± 3 nm to 30 ± 5 nm by increasing the GI time from 0 s to 2 min. It is important to notice that, for this material system, the AFM is a good probe of morphological characteristics of the QDs, since the AlN capping modifies the strain state of the QDs, but it does not significantly alter the QD shape.[11] To guarantee that the GaN islands on the surface are not subject to additional ripening, the samples were rapidly quenched to room temperature immediately after the GI that follows the deposition of the last QD layer.

Photoluminescence (PL) experiments were carried out at room temperature using the UV excitation line ($\lambda=244$ nm) of a frequency-doubled continuous-wave Ar^+ laser. The PL signal was focused into a 0.46 m focal length monochromator, and detected with a charge coupled device camera. The PL peak energies, along with the corresponding FWHM for all samples, are reported in Table I. The inset of Fig. 2 shows the PL spectra of Samples E644, E648, and E649. The PL is peaked at energies ranging from 3.78 to 3.9 eV, which is typical of dots with a height of 4–5 MLs (1–1.3 nm).[13] The FWHM is in the range of 0.2–0.25 eV. This value is remarkably small for nitride QDs,[6] and it suggests a good size homogeneity.

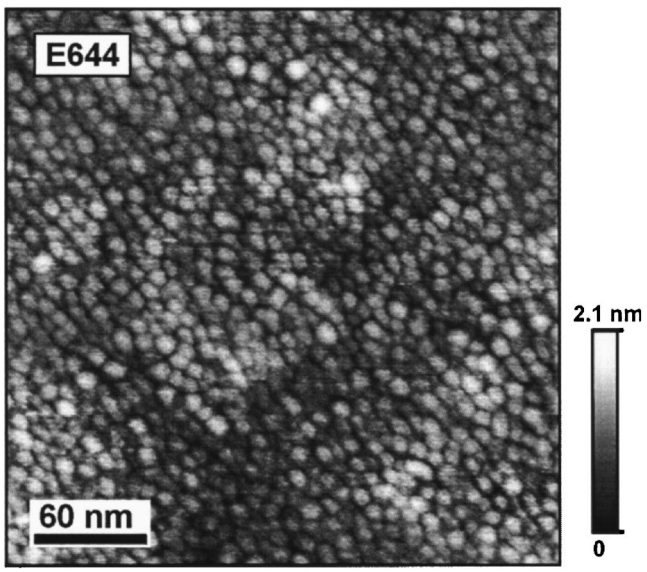

FIG. 1. AFM image of QDs on the surface of Sample E644 obtained in tapping mode using a Dimension 3100 system.

For the infrared (IR) absorption measurements, the samples were mechanically polished in a 45° multipass waveguide geometry with 4–5 total internal reflections. The IR transmission for *p*- and *s*-polarized light was measured at room temperature using a Fourier transform IR spectrometer and a deuterated triglycine sulfate photodetector. Figure 2 shows the absorption of Samples E644 and E649 for *p* polarization and of Sample E648 for *p* and *s* polarizations. These QD samples exhibit *p*-polarized absorption peaked between 0.81 eV (1.53 μm) and 0.878 eV (1.41 μm). As seen in Fig. 2, no absorption is observed for *s*-polarized light within experimental accuracy. The oscillating feature arises from Fabry–Perot interferences in the epitaxial layers and AlN buffer. The *p*-polarized interlevel absorption energy of all studied samples, along with the corresponding FWHM, is reported in Table I. For the sample grown with shorter GI, the interlevel transition is peaked at higher energies. This is in agreement with the smaller QD size measured by AFM. The FWHM is as low as 88 meV for Sample E649. Based on

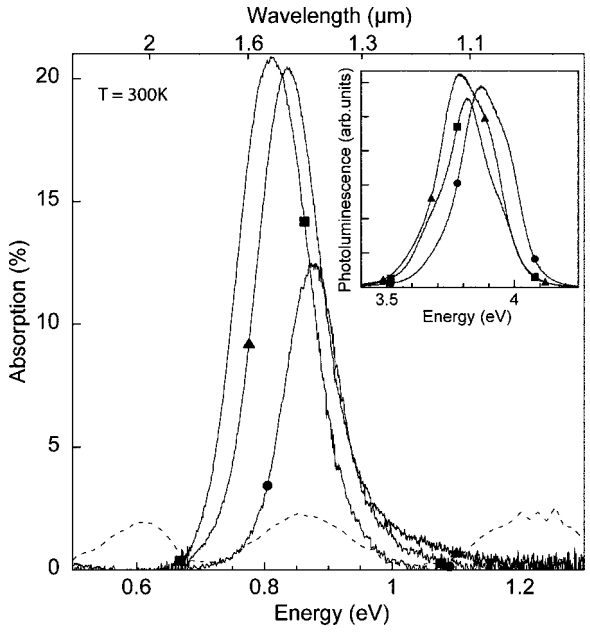

FIG. 2. Room-temperature intraband absorption of Samples E644 (full line with triangles), E648 (full line with squares), and E649 (full line with circles) for *p*-polarized light and of Sample E648 (dashed line) for *s*-polarized light. The measurements were performed in a multipass waveguide configuration with four internal reflections. Inset: Room-temperature PL spectra for Samples E644, E648, and E649.

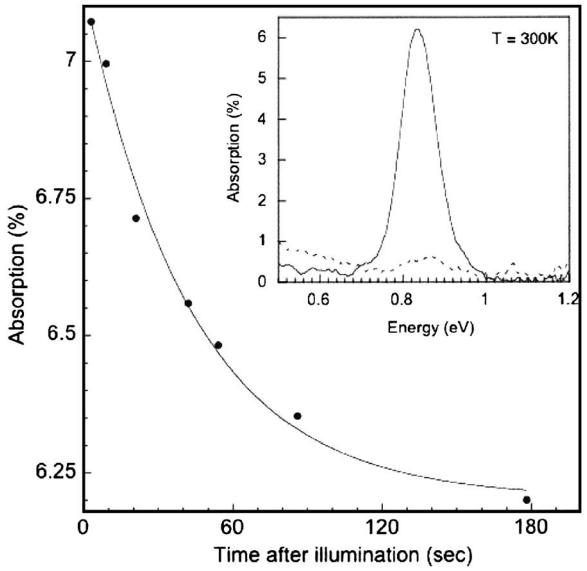

FIG. 3. Decay of the absorption of Sample E645 after UV illumination: The full circles are the experimental points, while the full curve is an exponential fit with a decay time of 43 s. Inset: Interlevel absorption of Sample E645 for *p*- (full line) and *s*- (dashed line) polarized light.

our previous findings,[6] we attribute the *p*-polarized peak to the transition from the ground state (*s*) to the excited state confined along the *c* axis (p_z). The fundamental absorption of the dots from the ground state *s* to the in-plane excited states (p_x or p_y) is not observed because it probably occurs below the cut-off energy of the substrate,[14,7] located at 0.3 eV ($\lambda = 4.1\ \mu$m). However, one cannot exclude that the s-p_x and s-p_y absorption for heavily doped samples is vanishingly small due to the excited state filling.

The thickness and length of the multipass waveguides was set to allow four to five internal reflections. Under these conditions, the samples that were *n* doped to 1×10^{20} cm^{-3} exhibit an absorption in the 12.4–20.8% range. For comparison purposes, the per-reflection absorption (i.e., the measured absorption divided by the number of total internal reflections) is summarized in Table I for all the investigated samples. Although the absorption increases with doping, its trend is not linear. In addition, Sample E645—which is nominally undoped—shows a weak *p*-polarized absorption peaked at 0.823 eV (1.51 μm) with a FWHM of 94 meV (see Fig. 3, inset).

The latter unexpected finding cannot be explained by the GaN residual doping, which is estimated to be $\sim10^{17}$ cm^{-2} and, therefore, it is too weak to provide a detectable electronic population. One possible explanation is the efficient trapping of electrons in the dots from impurity states located in the AlN barriers. It is well known that oxygen is a common substitutional impurity which can be present in large concentrations in AlN. The incorporation of oxygen in AlN leads to a deep-defect band with a broad energy range from $\approx$0.7 eV to $\approx$2.7 eV below the conduction band of AlN.[15] It is expected that the deep levels—with an energy higher than that of the QD ground state, typically 1 eV below the AlN conduction band—are responsible for the population of the dots. Deeper levels can also be activated for example using light illumination. Indeed, we have observed that the interlevel absorption of Sample E645 (and of all the doped samples, too) increases under illumination by either a UV or a visible argon laser. Furthermore, after illumination, the interlevel absorption returns to its initial value of 6.2% within a few minutes. Figure 3 shows a typical absorption decay after sample illumination. A decay time constant of $\sim$43 s is estimated using the exponential fit. Such a long recovery time is in agreement with a simplified model where electrons photoexcited from deep defects in the AlN barriers are then captured by the QDs. The extremely long lifetime stems from the spatial separation between the donors, located in the AlN barriers, and the electrons efficiently trapped in the QDs. We stress that the unintentional doping of the AlN layer is difficult to control and this fact may explain the observed dispersion of interlevel absorptions for the doped samples.

In conclusion, we have reported the growth of high-density Si-doped self-organized GaN/AlN QDs displaying conduction-band interlevel absorptions at telecommunication wavelengths. The Si-doped QD absorption is shown to be dependent on the growth interruption time. Nominally undoped samples show residual intraband absorption as well as light-activated absorption, which are attributed to the detrapping of electrons in the AlN barriers and subsequent capture in the dots.

The authors would like to acknowledge A. Lusson and B. Daudin for fruitful collaborations as well as the financial support of EC FP6 STREP Project "Nitwave" under IST Contract No. 004170.

[1] C. Gmachl, H. M. Ng, S.-N. G. Chu, and A. Y. Cho, Appl. Phys. Lett. **77**, 3722 (2000).
[2] C. Gmachl, H. M. Ng, and A. Y. Cho, Appl. Phys. Lett. **79**, 1590 (2001).
[3] K. Kishino, A. Kikuchi, H. Kanazawa, and T. Tachibana, Appl. Phys. Lett. **81**, 1234 (2002).
[4] N. Iizuka, K. Kaneko, and N. Suzuki, Appl. Phys. Lett. **81**, 1803 (2002).
[5] A. Helman, M. Tchernycheva, A. Lusson, F. H. Julien, Kh. Moumanis, G. Fishman, E. Monroy, B. Daudin, D. Le Si Dang, E. Bellet-Amalric, and D. Jalabert, Appl. Phys. Lett. **83**, 5196 (2003).
[6] K. Moumanis, A. Helman, F. Fossard, M. Tchernycheva, A. Lusson, F. H. Julien, B. Damilano, N. Grandjean, and J. Massies, Appl. Phys. Lett. **82**, 868 (2003).
[7] A. Helman, F. Fossard, M. Tchernycheva, K. Moumanis, A. Lusson, F. Julien, B. Damilano, N. Grandjean, J. Massies, C. Adelmann, B. Daudin, and D. Le Si Dang, Physica E (Amsterdam) **17**, 60 (2003).
[8] A. Helman, M. Tchernycheva, K. Moumanis, A. Lusson, F. H. Julien, F. Fossard, E. Monroy, B. Daudin, D. Le Si Dang, B. Damilano, and N. Grandjean, Phys. Status Solidi C **1**, 1456 (2004).
[9] B. Daudin, F. Widmann, G. Feuillet, Y. Samson, M. Arlery, and J. L. Rouvière, Phys. Rev. B **56**, R7069 (1997).
[10] J. Brown, F. Wu, P. M. Petroff, and J. S. Speck, Appl. Phys. Lett. **84**, 690 (2004).
[11] V. Chamard, T Schülli, M. Sztucki, T. H. Metzger, E. Sarigiannidou, J.-L. Rouvière, M. Tolan, C. Adelmann, and B. Daudin, Phys. Rev. B **69**, 125327 (2004).
[12] E. Sarigiannidou, E. Monroy, B. Daudin, J. L. Rouvière, and A. D. Andreev, Appl. Phys. Lett. (to be published).
[13] V. Ranjan, G. Allan, C. Priester, and C. Delerue, Phys. Rev. B **68**, 115305 (2003).
[14] A. D. Andreev and E. P. O'Reilly, Phys. Rev. B **62**, 15851 (2000).
[15] G. A. Slack, L. J. Schowalter, D. Morelli, and J. A. Freitas Jr., J. Cryst. Growth **246**, 287 (2002).